# Constant Shape Factor Frequency Modulated Charge Pumping (FMCP)

J.T. Ryan[1], J.P. Campbell[1], J. Zou[1,2], K.P. Cheung[1], R.G. Southwick[3], A.S. Oates[4], and R. Huang[2]
[1]Semiconductor and Dimensional Metrology Division, NIST, Gaithersburg, MD 20899 USA
[2]Dept. of Microelectronics, Peking University, Beijing 100871, China
[3]IBM Research, Albany, NY USA
[4]TSMC, Hsin-Chu 30844, Taiwan, R.O.C.

*Abstract*— **We examine the seemingly frequency-dependent gate leakage current component of frequency-modulated charge pumping and show it to be a measurement artifact. If untreated, this results in erroneous defect density extractions. We present a constant shape factor methodology to suppress this component such that frequency-modulated charge pumping is well positioned for advanced device defect characterization.**

## INTRODUCTION

The increase in gate leakage current in advanced devices has become so troublesome that even the most utile device characterization techniques, like charge pumping [1-5], are becoming increasingly unworkable [5]. This poses a serious issue for modern technology development. Defect monitoring feedback tools, such as charge pumping, are becoming increasingly more important to keep development costs down and helping to bring products to market faster.

Simply speaking, when the gate leakage becomes large compared to the charge pumping signal, the precision in which the charge pumping signal can be measured is detrimentally reduced [6]. Compounding this precision issue are the very small numbers of defects present in highly scaled devices. Since single digit populations of defects matter in highly scaled devices, even modest precision issues can introduce significant error in defect density extractions. Furthermore, gate leakage current is only getting worse with each new technology generation.

The most obvious approach to deal with the precision issues is to increase the magnitude of the charge pumping signal by increasing the charge pumping frequency. Since charge pumping current is directly proportional to charge pumping frequency [1-3], a higher frequency results in a larger charge pumping current relative to the gate leakage background. Efforts utilizing this approach have extended charge pumping to very high frequencies [7-11] including GHz sine wave gate voltage waveforms [9, 10] and GHz square waves [11]. However, such charge pumping frequencies introduce incomplete trap filling concerns causing an ambiguous decreases in charge per cycle (and hence errors in defect density extraction) [12]. Utilization of sine waveforms equates to a gate voltage that, by definition, is always changing. Since the device never reaches an equilibrium or quasi equilibrium state, emission loss also becomes a concern.

By far, the most common and experimentally accessible charge pumping approach to handle excessive gate leakage involves the subtraction of two successive charge pumping measurements at different frequencies [5]. In this approach, gate leakage is assumed frequency independent [5]. By subtracting two charge pumping measurements taken at different frequencies, the gate leakage components are removed leaving a pure charge pumping signal. Unfortunately, this approach also begins to break down when the charge pumping signal is small compared to the leakage background [6]. Subtracting two large numbers (charge pumping signal with leakage) with the hopes of extracting a small number (charge pumping signal) is a difficult endeavor which faces the same precision issues mentioned earlier. The assumption of frequency independent gate leakage is indeed intuitive, but as will be discussed later, a questionable assumption.

In our previous work [6], a highly modified version of the two-frequency subtraction technique was developed in which the gate waveform consists of a frequency-modulated square wave. In the simplest sense, the frequency-modulated charge pumping (FMCP) technique is identical to the above discussed two frequency subtraction technique. The key advancement is a much more practical signal detection scheme which transforms the traditional DC charge pumping approach into an AC detected measurement. In such an AC detected scheme, the measurements immunity to high levels of leakage is greatly enhanced.

Fig.1 illustrates the schematic measurement arrangement for FMCP. The MOSFET device-under-test source and drain terminals are grounded while a frequency-modulated gate voltage is applied to the gate. The current through the substrate is measured via a digital storage oscilloscope or, more ideally a lock in amplifier. Further details and discussion can be found in [6].

As previously mentioned, the FMCP measurement transforms the conventional quasi-DC measurement to an AC measurement of the difference between charge pumping currents at two different frequencies. This AC arrangement lends itself to significant sensitivity and precision improvements. The FMCP approach vastly suppresses the residual leakage background towards more manageable levels, as demonstrated in the Elliot curves [4] of fig. 2. However, a careful examination of fig. 2 reveals a smaller, seemingly frequency-dependent, leakage current component most noticeable when the gate voltage pulse is shifted towards inversion (right hand side of fig. 2). What are the origins of this seemingly frequency-dependent leakage current? Does it impact earlier FMCP results? Can it be avoided?


978-1-4799-0352-8/13/$31.00 ©2013 IEEE

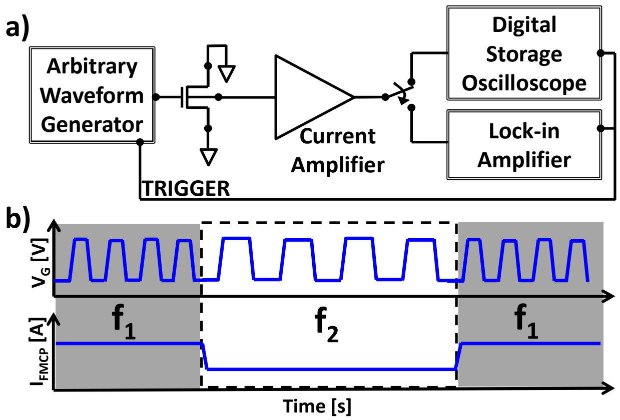


Fig. 1: (a) Schematic representation of the frequency modulated charge pumping (FMCP) measurement. An arbitrary waveform generator applies a frequency-modulated square wave voltage pulse to the gate electrode. The AC-coupled substrate current is measured with a current amplifier and a digital storage oscilloscope or lock-in amplifier. (b) The measured FMCP current oscillates between the two different modulation frequencies. The difference between these two different currents ($\Delta I_{FMCP}$) corresponds to charge pumping at the difference of the two frequencies.

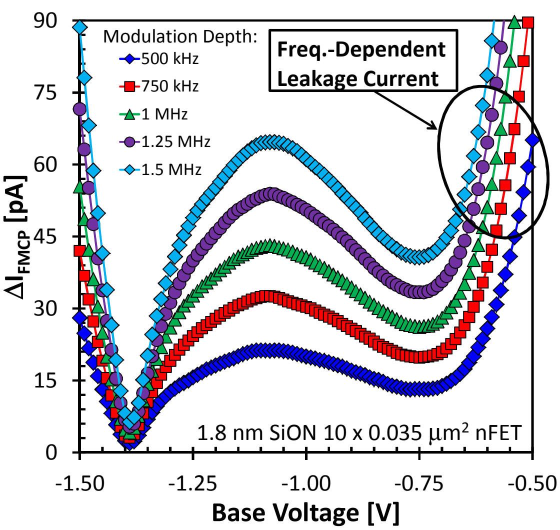


Fig. 2: FMCP vs. base voltage (Elliot curve) for a 1.8nm SiON 10 x 0.035 $\mu m^2$ nFET. The amplitude of the square wave gate waveform is 1.8 V and the center frequency (value around which the frequency is modulated) is 3 MHz. Note the seemingly frequency-dependent leakage current which dominates the measured substrate current at higher base voltages in inversion.

## DISCUSSION

The origin of the frequency-dependent leakage current can be best understood through a deeper examination of (1) the applied gate waveform and (2) the gate to substrate leakage ($I_{substrate}$-$V_G$) characteristic shown schematically in fig. 3. Since we are interested in the gate leakage current which impacts the charge pumping current, we are careful to use the gate to substrate leakage current (not just the gate current). From fig. 3, it is clear that the leakage current is most dominant during the static high and low time portions of the gate voltage pulse period (to first order). The asymmetry in the leakage characteristic necessarily results in a non-zero leakage current observable in the charge pumping current. In FMCP [6], or any two-frequency charge pumping measurement such as the two frequency subtraction method [5], the total time spent in either the high or low portions of the voltage pulse becomes frequency-dependent. Specifically, as the frequency increases *less* time is spent in both the high or low voltage portions and *more* time is spent in transition. This is an error which has long been overlooked and calls into question the previously discussed assumption of frequency independent leakage current in charge pumping.

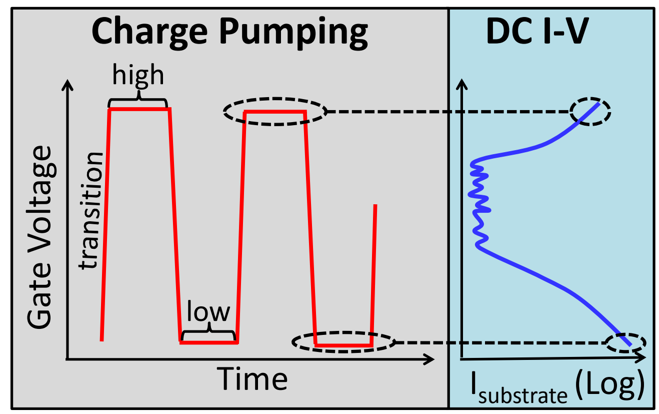


Fig. 3: Schematic illustration comparing the DC $I_{substrate}$-$V_G$ characteristic (right) and the charge pumping gate voltage wave form (left). This clearly shows that the maximum substrate leakage current in the charge pumping measurement occurs during the pulse high and low times and is less important for the transition times. As the frequency increases, less time is spent in high and low while more time is spent in a transition.

This frequency-dependent leakage current component is further explored through a series of simple calculations. In these calculations, the pure charge pumping current [1-3] is given by $I_{CP} = qAfN_{it}$ with $N_{it}$ = $10^{10}$ /cm$^2$ where $I_{CP}$ is the charge pumping current, $q$ is electronic charge, $A$ is the device area, $f$ is the charge pumping frequency and $N_{it}$ is the area density of interface defects. Note that we assume the measurement is probing the entire band gap (full accumulation to full inversion) and hence a probed energy window and energy distribution of defects ($D_{it}$) [1-3] is not included.

The leakage current is calibrated by integrating charge with respect to time for one waveform period using the measured $I_{substrate}$-$V_G$ characteristic from a 1.8 nm SiON 1 x 0.5 $\mu m^2$ nMOSFET, as illustrated in fig. 4.

These charge pumping current and leakage calculations yield the expected frequency-dependent gate leakage component (decreases with increasing frequency) which clearly impacts the net $I_{CP}$ vs. frequency slope and consequent extracted defect density, as shown in fig. 5. We note that this effect is exacerbated for (1) longer rise/fall times and (2) larger DC leakage current asymmetry. The absolute value of the leakage current in these calculations is based solely on the leakage current in the calibration device.

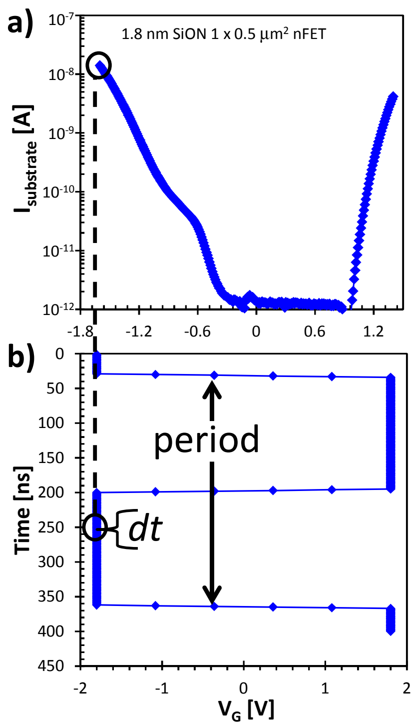


$$I_{Leakage} = \frac{1}{period} \sum_{time} I_B(V_G) x\, dt(V_G)$$

Fig. 4: Illustration of the procedure to calculate the expected charge pumping leakage current from (a) DC $I_{substrate}$-$V_G$ characteristic curve taken on a 1.8 nm SiON 1 x 0.5 µm$^2$ nFET and (b) knowledge of the gate wave form. $I_{substrate}$ was measured with $V_S = V_D = V_B = 0$ V.

To treat this obstacle and remove this frequency dependent leakage current, we introduce the concept of a constant shape factor, illustrated in fig. 6. In this approach, the high time/rise time and low time/fall time ratios are kept constant as the frequency changes. This restriction necessarily forces equivalent total high and low times for each frequency (by compensating with rise/fall times) and insures that the gate leakage current is frequency-independent. For example a 2 MHz square wave with 5 ns rise /fall time yields a ratio of: 250 ns / 5 ns = 50. The constant shape factor restriction dictates then that a complementary 1 MHz square wave should have: 500 ns / 50 = 10 ns rise /fall time. In this way the frequency induced difference in high and low times are compensated by a change in rise/fall time. It should be noted that by definition, a sine wave has constant shape factor versus frequency. The negative implications of using sine wave gate voltages (discussed earlier in the text) outweigh the possible benefits of its constant shape factor properties.

More importantly, this insures a correct $I_{CP}$ vs. frequency slope (which is proportional to defect density) and an insensitivity to rise / fall times, as illustrated in fig. 7. Note that varying the rise/fall times excessively will, in principle, alter the probed energy window within the band gap [3] due to charge pumping emission loss. However, the typical rise/fall time variations required for constant shape factor implementation in advanced device structures (a few ns) introduces an extremely minor change in energy window.

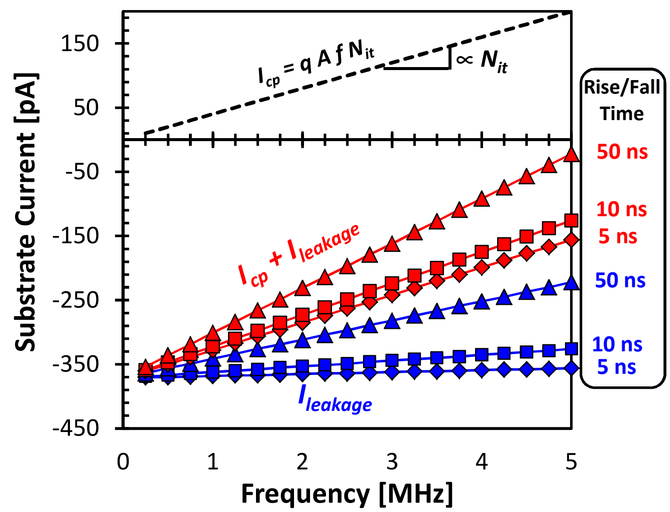


Fig. 5: Calculation of the frequency-dependent gate to substrate leakage current ($I_{leakage}$) and its impact on the measured charge pumping current ($I_{CP}$). Note that the frequency-dependent leakage current induces a change in slope which erroneously affects the extracted defect density ($N_{it}$). This effect is exacerbated for longer rise/fall times.

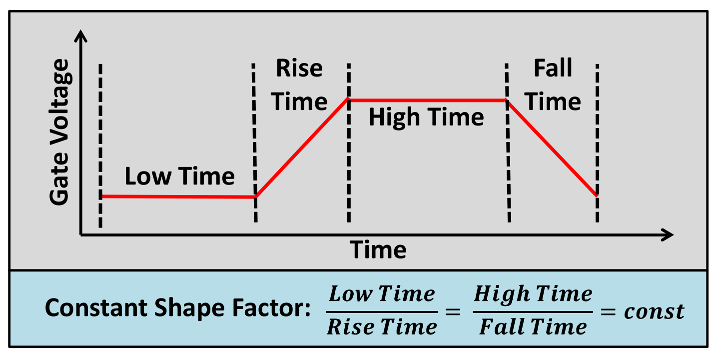


Fig. 6: Enforcing a pulse shape with the constant shape factor restriction ensures that the total time spent in either the high or low state is frequency independent.

In principle, it would seem that an experimental implementation of this constant shape factor charge pumping would ensure proper FMCP results and further extend the technique's utility. However, implementation of the constant shape factor requires precise control (sub-ns range) of the pulse shape. This high level of precision is proportional to the magnitude of the leakage current. Unfortunately, this is a feature which is absent from the majority of commercially available arbitrary waveform generators. Provided that one does not have access to the necessary arbitrary waveform generator, the easiest experimental implementation of constant shape factor involves an arrangement similar to the one schematically shown in fig. 8. We note that this arrangement is consistent with a constant shape factor, but does not allow for completely ideal waveform shape control mainly due to the timing restrictions of the source waveform generators.

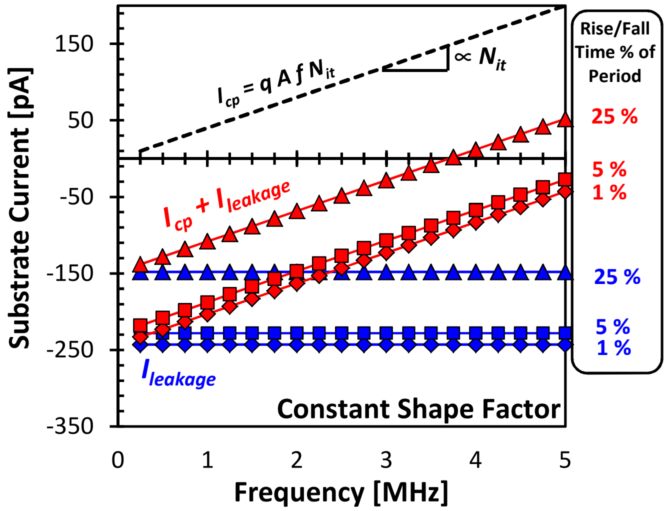


Fig. 7: Calculation illustrating the frequency independence of the gate to substrate leakage current ($I_{leakage}$) when the constant shape factor restriction is enforced. In this case, the leakage introduces a frequency-independent shift in the net substrate current which allows for accurate defect density extraction. Note that once the constant shape factor restriction is enforced, there is no sensitivity to the rise and fall times.

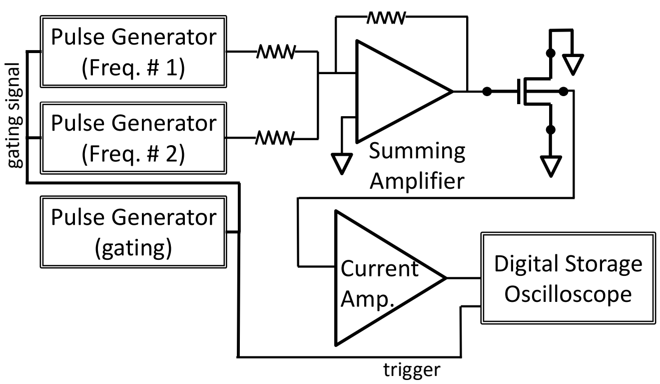


Fig. 8: In this (quasi-constant shape factor) FMCP experimental arrangement, two pulse generators are operated in burst mode and supply the necessary waveforms for (frequency 1 and frequency 2). A third signal source acts to sequentially gate off the two pulse generators such that the transition between frequency 1 and frequency 2 is seamless (this also controls the modulation frequency). For proper impedance matching the two waveform sources are summed together using a simple op-amp circuit. The substrate FMCP current is collected using a current amplifier and a digital storage oscilloscope or a lock in amplifier (not shown).

Quasi-constant shape factor FMCP is experimentally demonstrated for a 1.8 nm SiON 1 x 0.06 $\mu m^2$ nMOSFET using the constant shape factor circuit and is shown in fig. 9. Notice that the frequency dependence of the gate leakage current is greatly suppressed for larger values of $V_{base}$ (the problem region in fig. 2). This is a good indicator that the extracted defect density is relatively free from error. This result also demonstrates the utility of constant shape factor FMCP to probe highly-scaled device geometries with exceedingly small numbers of defects.

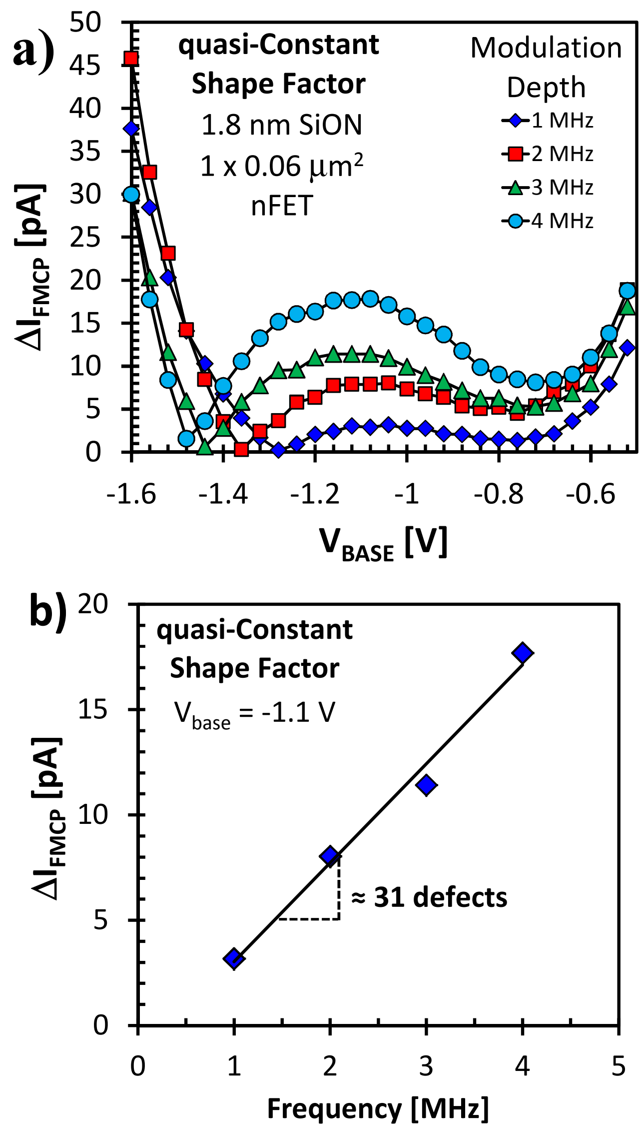


Fig. 9: (a) Quasi-constant shape factor FMCP results for a 1.8 nm SiON 1 x 0.06 $\mu m^2$ nFET using the experimental arrangement from fig. 8. The gate waveform amplitude was 1.8 V. Notice the suppression of the frequency dependent leakage current at higher values of base voltage. The frequency dependent $N_{it}$ extraction (b) indicates that this technique is well equipped to extend charge pumping's range to highly scaled (and highly leaky) advanced device nodes.

## CONCLUSIONS

In summary, FMCP's ability to salvage charge pumping on very leaky devices unintentionally introduces a frequency-dependent gate leakage component which can, in most instances, alter the extracted defect density values. Assurance of a constant shape factor gate waveform eliminates this issue, although it requires a somewhat advanced experimental arrangement.

## REFERENCES

[1] J. S. Brugler and P. G. A. Jespers, "Charge pumping in MOS Devices," *IEEE Trans. Electron Devices*, vol. 16, no. 3, pp. 297-302 (1969).

[2] G. Groeseneken, H.E. Maes, N. Beltran, and R.G. DeKeersmaecker, "A reliable approach to charge pumping measurements in MOS transistors," *IEEE Trans. Electron Devices*, vol. 31, no. 1, pp. 42-53 (1984).

[3] G. Van Den Bosch, G.V. Groeseneken, P. Heremans, and H.E. Maes, "Spectroscopic charge pumping: A new procedure for measuring interface trap distributions on MOS transistors," *IEEE Trans. Electron Devices*, vol. 38, no. 8, pp. 1820-1831 (1991).

[4] A.B.M. Elliot, "The use of charge pumping currents to measure surface state densities in MOS transistors," *Solid-State Elec.*, vol. 19, pp. 241-247 (1976).

[5] P. Masson, J.L. Autran, and J. Brini, "On the tunneling component of charge pumping current in ultrathin gate oxide MOSFETs," *IEEE Elec. Dev. Lett.*, vol. 20, no. 2, pp. 92 – 94 (1999).

[6] J.T. Ryan, J.P. Campbell, K.P. Cheung, J.S. Suehle, R.G. Southwick, and A.S. Oates, "Reliability monitoring for highly leaky devices," *Proc. of the IEEE Intl. Reliab. Phys. Symp.*, pp. 2D.5.1 – 2D.5.4 (2013).

[7] R. Fernandez, B. Kaczer, A. Nackaerts, S. Demuynck, R. Rodriguez, M. Nafria, and G. Groeseneken, "AC NBTI studied in the 1 Hz – 2 GHz range on dedicated on-chip CMOS circuits," *IEEE Intl. Elec. Dev. Meeting* (2006).

[8] M. Cho, B. Kaczer, M. Aoulaiche, R. Degraeve, P. Roussel, J. Franco, T. Kauerauf, L.A. Ragnarsson, T.Y. Hoffmann, G. Groeseneken, "Interface trap characterization of a 5.8 angstrom EOT p-MOSFET using high-frequency on-chip ring oscillator charge pumping technique," *IEEE Trans. Elec. Dev.*, vol 58, no. 10, pp. 3342-3349 (2011).

[9] G.T. Sasse and J. Schmitz, "Charge pumping at radio frequencies: methodology, trap response and application," *Proc. of the IEEE Intl. Reliab. Phys. Symp.*, pp. 627 – 628 (2006).

[10] G.T. Sasse and J. Schmitz, "Application and evaluation of the RF charge pumping technique," *IEEE Trans. Elec. Dev.*, vol. 55, no. 3, pp. 881-889 (2008).

[11] Y. Wang and K.P. Cheung, "Carrier capture at the $SiO_2$-Si interface: a physical model," *Appl. Phys. Lett.*, 91, 113509 (2007).

[12] J.T. Ryan, L.C. Yu, J.H. Han, J.J. Kopanski, K.P. Cheung, F. Zhang, C. Wang, J.P. Campbell and J.S. Suehle, "Spectroscopic charge pumping investigation of the amphoteric nature of $Si/SiO_2$ interface states," *Appl. Phys. Lett.*, 98, 233502 (2011).